Effects of Extractor Axial Position on Porous Ionic Liquid Ion Source Performance

IEPC-2022-194

Presented at the 37th International Electric Propulsion Conference
Massachusetts Institute of Technology, Cambridge, MA, USA
June 19-23, 2022

T. Kerber[1], H. Sargent[2], and K. Lemmer[3]
Western Michigan University, Kalamazoo, MI, 49007, United States

C. Ryan[4]
University of Southampton, Southampton, Hampshire, SO17 1BJ, United Kingdom

A porous-media type, passively-fed, single emitter ionic liquid ion source electrospray thruster with variable extractor electrode to emitter axial distance was tested. Plume current-voltage curves and extractor current-voltage curves were measured for extractor to emitter distances from -0.1 mm (below emitter apex) to +0.5 mm (above emitter apex). After onset, the formation of a secondary and tertiary emission site was identified via step change in current and shift in current-voltage slope. Results show a linear increase in onset voltage with increasing emitter-extractor distance and a reduction in slope of the plume current to applied voltage curve, with extractor positions below the emitter having the highest current to voltage slope. Temporally-resolved plume current and extractor current behaviour in the onset voltage region was also examined. A time delay between applied potential and plume current emission of 0.48 s at the initial onset voltage of 2070 V decreased to zero after 2160 V when the extractor was co-planar with the emitter tip. This ΔV_t between first delayed emission and immediate emission remained constant as the extractor was moved downstream of the emitter.

I. Nomenclature

I_{ex}	=	Current measured on the extractor electrode
I_{pl}	=	Plume current measured on the downstream collector electrode
Δt	=	Time delay between full-scale applied potential and ion emission
V_o	=	Onset voltage at which emission is detected on the collector electrode
V_{em}	=	Voltage of potential applied to the distal electrode
η_{tr}	=	Transmission efficiency

II. Introduction

The electrostatic evaporation and acceleration of charged particles from a fluid, referred to as electrospraying, is used in a wide array of applications from mass spectrometry [1] to microelectromechanical systems (MEMS) manufacturing and is being developed for in-space electric propulsion (EP) for micro/nanosatellites [2], high-precision pointing [3], and accurate attitude control [4]. As a propulsion device, the electrospraying process has been implemented in different forms, including a capillary tube [5], an externally-wetted roughened needle [6], and a porous cone [7]. Passively-fed

[1]Ph.D. Candidate, Mechanical and Aerospace Engineering, thomas.v.kerber@wmich.edu
[2]Master's Student, Mechanical and Aerospace Engineering, hannah.g.sargent@wmich.edu.
[3]Associate Professor, Mechanical and Aerospace Engineering, kristina.lemmer@wmich.edu
[4]Lecturer, Aeronautics and Astronautics, c.n.ryan@soton.ac.uk.

electrosprays that emit in the pure-ionic regime (PIR) have received particular focus in EP development due to their potential for high efficiency (>90%), high specific impulse (>1000 s), low noise, and high accuracy thrust [8]. The transition from metallic emitters to dielectric emitter materials, such as borosilicate glass, along with the use of upstream distal grids and bipolar potential operation has improved total impulse by reducing the electrochemical etching of the emitters and thus increasing lifetime [9, 10]. Additionally, the use of room temperature molten salt solutions called ionic liquids as the propellant, pioneered by de la Mora, has reduced onset voltage requirements and increased the rate of ion current emission per applied potential [11]. These advancements, along with the volume scaling down of communication and power systems, will enable capabilities of micro/nanosatellites previously only available to larger satellites.

Figure 1 depicts a simplistic diagram of a porous-media type electrospray with the ionic liquid saturated dielectric emitter, biased distal electrode, and grounded extractor electrode. With flight thruster development causing an increase packing density, and building larger emitter arrays to increase total thrust, maintaining uniform alignment between the extractor grid and emitter array across the thruster becomes an engineering challenge. The extractor electrode alignment with respect to the emitter is a key aspect of the thruster geometry that affects performance, including onset voltage, current on the extractor electrode from accelerated ions intercepting the grid, plume vector, and lifetime. Few studies in the literature exist experimentally examining the impact extractor-emitter positioning has on these parameters. By characterizing these effects with a single emitter, specific changes in geometry can be studied without the interference of an arrayed thruster with varied emitter geometries obscuring results.

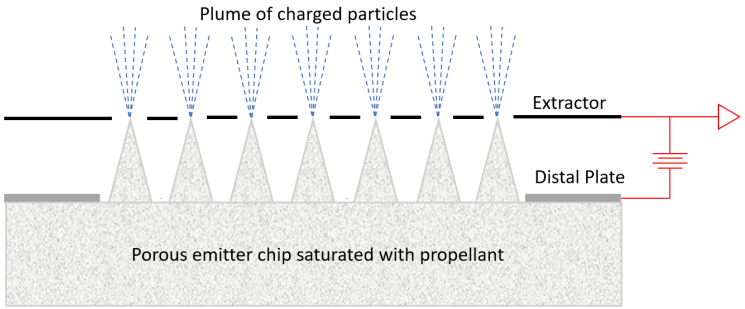

Fig. 1 Diagram of an array of porous-media type emitters for an pure-ionic regime electrospray thruster.

Transient behaviour of the plume current and extractor current during operation is another understudied phenomenon in PIR electrosprays. Transient behaviours during bipolar operation, which have been infrequently studied for porous media, dielectric single emitters, can affect lifetime and thruster performance. Huang et al. [12] performed studies on a porous nickel single emitter electrospray at several extractor positions downstream of the emitter. They observed plume current modes with delays between applied voltage and current emission that evolved as emitter voltage increased. This delay was attributed to the time required for fluid to accumulate in the Taylor cone. Schroeder et al. [6] also observed, for externally-wetted tungsten emitters, that there is a several millisecond delay in emission after voltage switching, as well as an overshoot in plume current which decays in under a millisecond. This results in inaccurate performance models and potentially unpredictable in-space operation. Transient characterization of the Busek BET-300-P also showed an overcurrent in the plume transients with a total rise time to steady-state of 15 ms [13]. Courtney et al. did not observe any overcurrent in the extractor, indicating that transient behavior may have less of an impact on lifetime for PIR electrosprays compared to colloidal electrosprays. However, this study was completed with an arrayed thruster, making precise characterization of these onset behaviours difficult.

A telemetry-based study of the performance of a single emitter, porous-media electrospray thruster as a function of extractor-emitter axial distance is discussed. This paper is divided into five sections, the experimental setup and thruster used for testing is described in Section III. Section IV presents the current-voltage (I-V) curves of the extractor and emitter in positive and negative polarity as a function of the distance between the extractor and emitter along with temporal data of the extractor and emitter current during transitional regimes. The paper ends with Section V presenting the conclusion and future work for this research.

III. Experimental Setup

A. Electrospray Thruster

P5 (1-1.6 μm average pore size) borosilicate glass CNC milled into a single 1.0-mm-tall cone was used as the emitter shown in Fig. 2. A P4 (10-16 μm) borosilicate chip spring loaded against the bottom of the emitter chip with a

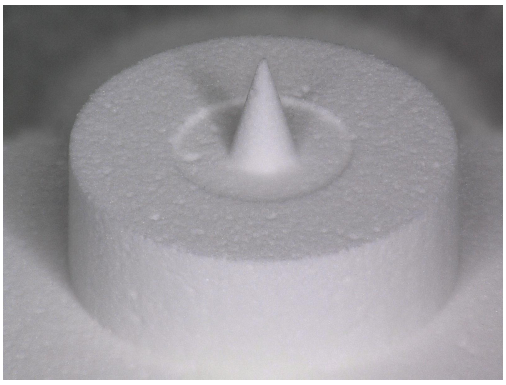

Fig. 2 Image of the type of porous borosilicate single emitter used during testing.

Whatmann filter paper #1 interface was used as a propellant reservoir and induced a Laplace back pressure to facilitate passive capillary flow to the emitter apex [14]. Electrical contact to the propellant was made with a stainless steel distal plate pressed against the top face of the emitter. The extractor electrode was machined from a 0.06-mm-thick molybdenum sheet, with a 1.4-mm-diameter orifice. The extractor was mounted above the emitter as shown in Figure 3 with a linear motion stage to enable in-vacuum axial positioning. The emitter was visually positioned concentric with the extractor orifice, with the "in-line" or zero position of the extractor-emitter system being where the apex of the emitter lies between the top and bottom surfaces of the extractor.

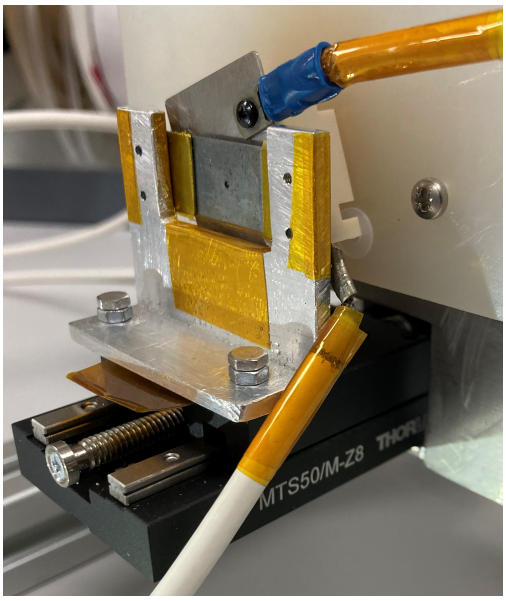

Fig. 3 Image of the electrospray thruster with linear motion stage for axial positioning of extractor electrode.

1-Ethyl-3-Methylimidazolium Tetrafluoroborate (EMI-BF_4) is a highly conductive ionic liquid with extensive use as an electrospray propellant [15–17]. EMI-BF_4 has high conductivity, high surface tension, and negligible vapor pressure making it an ideal ionic liquid for PIR electrospray operation. All experiments were completed with EMI-BF_4 that was

first outgassed below 1 Torr for several hours until gas bubbles stopped forming in the liquid. Propellant was first loaded into the reservoir and then the emitter was placed into a shallow dish with the propellant and returned to mTorr-level pressures for 12 hours for the propellant to fully saturate the porous glass.

B. Facility

Tests were completed at the David Fearn Laboratory in the Astronautics Group of the University of Southampton. A 0.6-m-diameter by 0.7-m-long vacuum chamber with a base pressure of 1.2×10^{-5} Torr, pumped with a Leybold Turbovac Mag 600 with 550 l/s N_2 was used for all testing. Single emitter experiments which have low mass flow rates combined with the pumping speed of the vacuum pump resulted in no noticeable difference in chamber pressure between thruster operation and base pressure. A high-speed, high-voltage amplifier from Matsuda Precision Inc. with ±20 mA, ±5 kV output was used to bias the distal grid.

Emitter voltage was measured by the Matsuda Precision analog voltage monitor output. Extractor current was measured by grounding the extractor through a resistor and measuring the voltage drop with a NI 9201 DAQ at 100 Hz. A molybdenum plate with negatively biased screen was placed 40-mm downstream of the thruster and connected to ground through a resistor to measure the plume current.

IV. Results & Discussion

A. Plume Current

The extractor was positioned from -0.1 mm below up to 0.5 mm above the emitter tip. I-V curves of the plume current and extractor current were collected at each position. The thruster was operated in bipolar mode at 0.5 Hz in voltage-controlled mode for all experiments. The voltage ranges at each position were inconsistent due to instabilities which occurred at lower potentials for closer extractor positions. Both shorting events and high, unstable, current on the extractor limited consistent voltage sweeps across all extractor positions.

Fig. 4 shows I-V curves of the plume current for each extractor position in both positive and negative polarity. The first discrete steps in current after onset at the -0.1 mm, -0.05 mm, in-line, and 0.1 mm positions likely indicate the formation of a secondary emission site. The slope of the I-V curve does not increase after this first current step. From this, it is inferred that the secondary site is poorly aligned with the extractor orifice and emission from this site is impeded. The second current step which indicates the presence of a tertiary emission site does increase the IV slope. At the higher extractor positions past 0.2 mm above the emitter, the formation of a secondary site is less apparent from the plume current data. A slight reduction in the I-V slope, without a current step, at 2520 V, 2740 V, and 2820 V, for the 0.3 mm, 0.4 mm, and 0.5 mm positions, respectively, does occur, potentially indicating the secondary site formed. However, thruster operation becomes unstable before the tertiary site with better alignment was able to form. For extractor positions past 0.1 mm there is an initial onset voltage which results in emission for approximately 60 V which then turns off. This can be seen in 4a at 2200 V (0.2 mm), 2420 V (0.3 mm), 2620 V (0.4 mm), and 2680 V (0.5 mm). This behaviour, along with the current steps and I-V slope changes indicating multiple emission sites is also seen in negative polarity operation when BF_4 is being emitted as seen in 4b.

From the results shown in Fig. 4, onset voltage was determined as the first voltage where measurable current above the noise was detected on the collector plate after the first temporary peak. Fig. 5 plots the onset voltage for both positive and negative polarities using the outlined method. Across this positional sweep, the onset voltage scales linearly for both positive and negative polarities and onset did not always occur at the same potential between the two. Typically, the negative polarity begins emission onset 20-40 V before the positive begins emitting.

Due to the formation of secondary and tertiary sites, which drove step changes in current and shifts in I-V scaling, it is difficult to fit a simple empirical scaling law to the I-V curves. However, qualitatively it can be observed that with the extractor in-line with the emitter, or below the emitter, I-V scaling is higher than with the extractor above the emitter. Comparatively, extractor positions above the emitter appear to be less sensitive to the extractor position, with no significant difference in slopes between the 0.2 mm, 0.3 mm, 0.4 mm, and 0.5 mm positions.

1. Transient Behavior

Time-resolved plume current measurements for the single emitter indicate a delay between ion emission and applied voltage before steady-state emission occurs. Unlike results presented by Huang et al. [12], only two current modes were observed. A delayed emission with initial transient peak and an immediate steady state mode. Fig. 6a shows an example

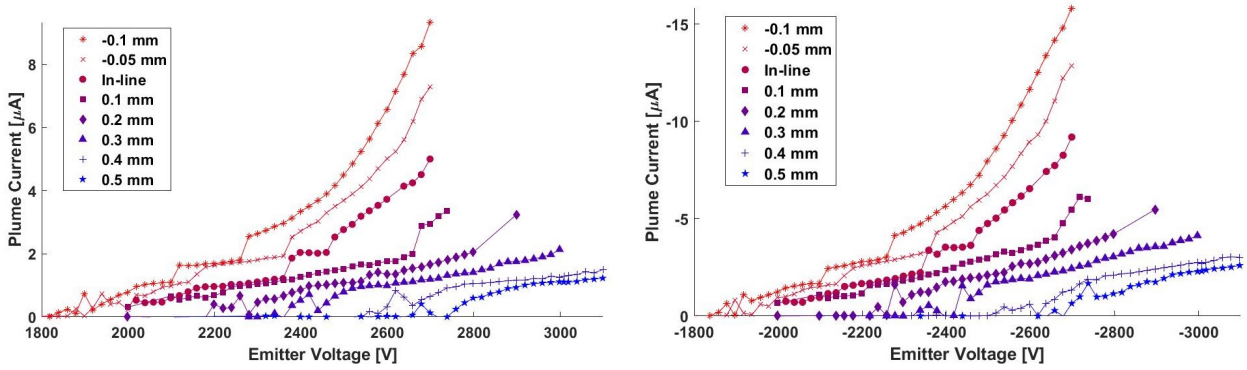

(a) Positive polarity plume current I-V curves. **(b) Negative polarity plume current I-V curves.**

Fig. 4 I-V curves of the collected plume current for the single emitter ionic liquid ion source at extractor to emitter distances from -0.1 mm to 0.5 mm.

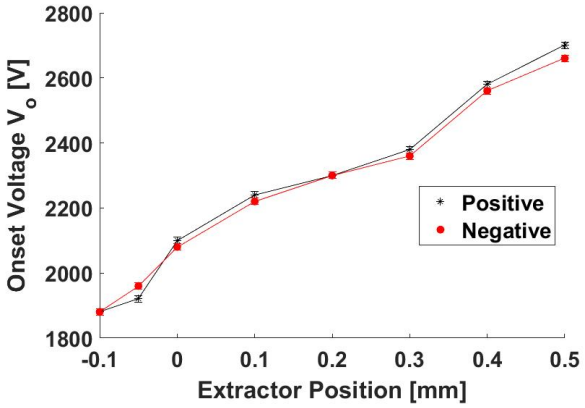

Fig. 5 Voltage at which current on the downstream collector is detected and continues to increase with increasing potential.

of the delayed emission mode with extractor in-line with emitter at 2060 V. As the emitter potential is increased this delay between applied voltage and ion emission, along with the current spike, approaches zero as shown in Fig. 6d with the same extractor position but at 2160 V. Potential sweeps near the onset voltage of the in-line and downstream extractor positions were completed with voltage increments of 10 V to better capture progression of the time delay between applied potential and emission. Results for both the positive and negative polarities are plotted in Fig. 7. The rate at which the time delay decreases with increasing voltage does not appear to be affected by the extractor positioning. The voltage sweep for the 0.4 mm position was terminated before the steady-state emission mode was reached.

For an arrayed electrospray, not all emitters have the same onset voltage due to varied emitter geometries. If the thruster is operated at a voltage were some emitters are operating in this regime, emission from those sites will contribute to unsteady thruster performance. More data are needed to determine if this phenomenon occurs for the secondary and tertiary sites.

B. Extractor Current

Fig. 8 plots the measured extractor current I-V curves at each extractor position. At voltages corresponding to the onset of the secondary site from the plume data, no significant increase in extractor current is observed. Since the secondary site caused a step change in the plume current but not an increase in scaling, it had minimal impact on the extractor current. Whereas, the onset of the tertiary site results in a significant increase in extractor I-V slope. The plume data provided no indication of a tertiary site for the 0.3 mm, 0.4 mm, and 0.5 mm positions; however, the extractor data shows a rapid increase in current at 2800 V, and 2900 V at those extractor positions. The outlying current data at -0.1

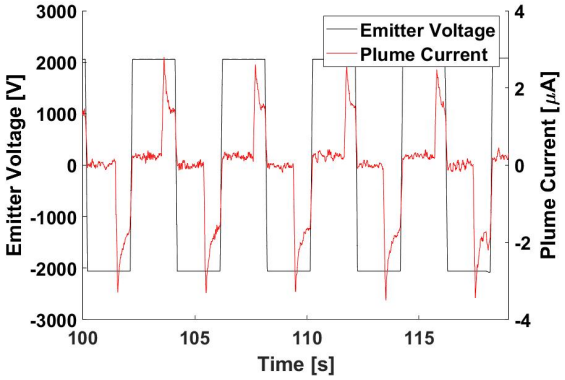

(a) Transient behavior of plume current near onset voltage at 2060 V.

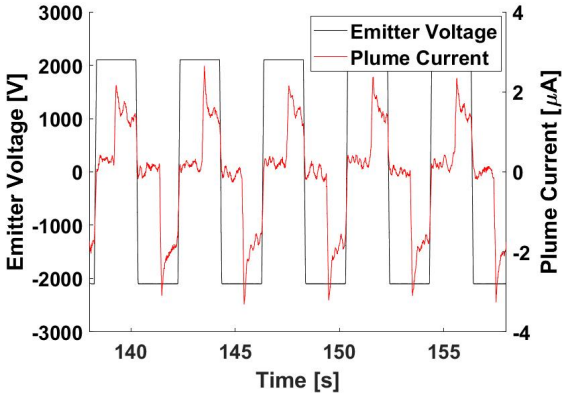

(b) Transient behavior of plume current near onset voltage at 2100 V.

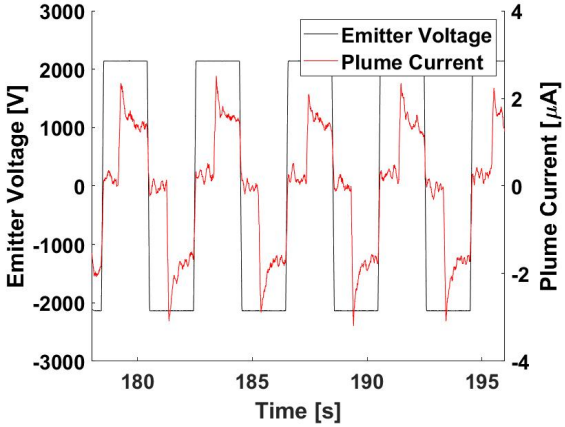

(c) Transient behavior of plume current near onset voltage at 2140 V.

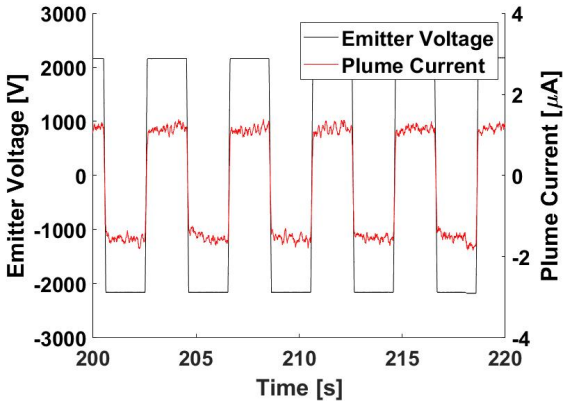

(d) Transient behavior of plume current near onset voltage at 2160 V.

Fig. 6 Time-resolved plume current and emitter voltage for in-line position of extractor showing evolution of current behavior near the onset voltage.

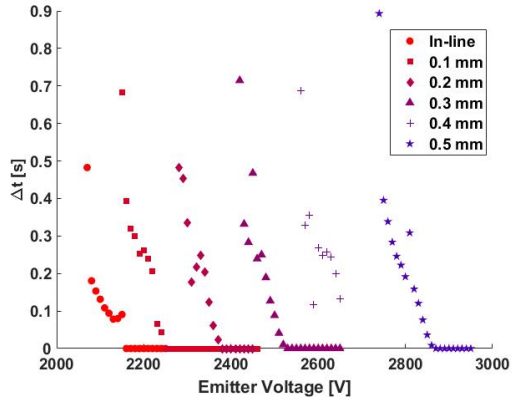

(a) Positive polarity

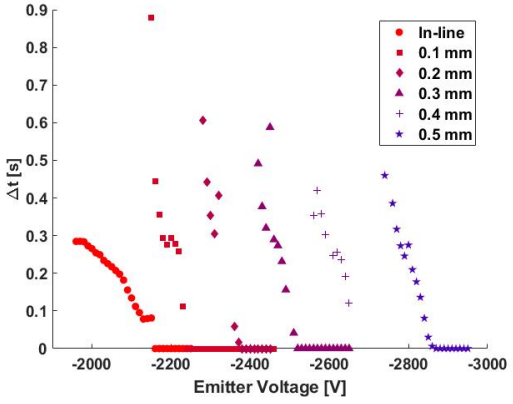

(b) Negative polarity.

Fig. 7 Evolution of plume current transient behavior as voltage is swept through the onset voltage.

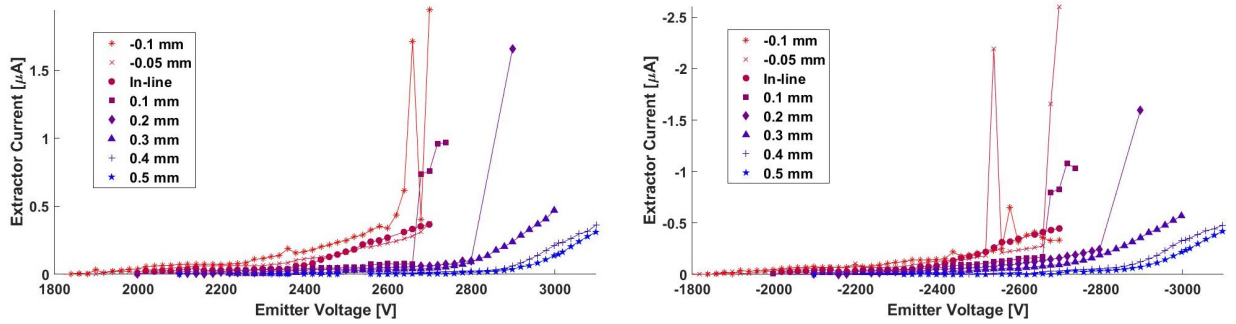

(a) Positive polarity **(b) Negative polarity.**

Fig. 8 I-V curves of the extractor current for the single emitter at extractor positions from -0.1-mm to 0.5-mm.

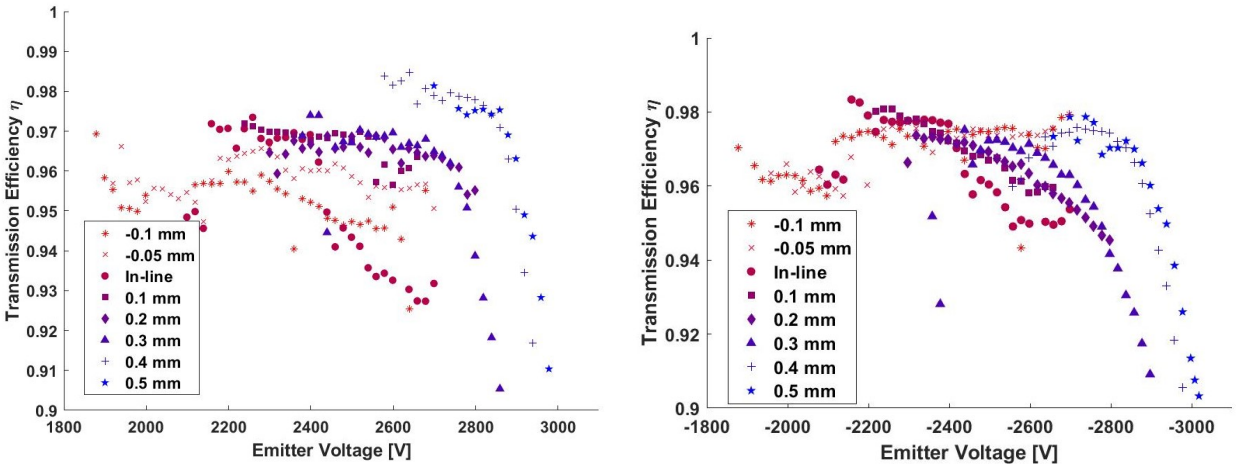

(a) Positive polarity **(b) Negative polarity.**

Fig. 9 Transmission efficiency at each extractor position starting at onset voltage.

mm, 0.1 mm, and 0.2 mm after 2600 V condition represents the beginning of the unstable operating regime previously discussed. At these same positions and potentials the plume current data showed no abnormally high emission while the extractor current experienced large fluctuations.

From the extractor current and plume current data, transmission efficiency was calculated using Eq. 1

$$\eta_{tr} = \frac{I_{pl}}{I_{pl} + I_{ex}} \tag{1}$$

where I_{pl} is the plume current and I_{ex} is the extractor current. Fig 9 plots the transmission efficiency as a function of voltage starting at the onset voltage for each extractor position. Results for transmission efficiency as a function of potential are chaotic with general treads being difficult to determine. In the literature, it is more common to present electrospray efficiencies at one or two nominal operating conditions instead of across the entire throttle range. One distinguishable feature is the reduction in efficiency at the 0.3 mm, 0.4 mm, and 0.5 mm positions after onset of the third emission site. Counter-intuitively, transmission efficiency was not shown to have a strong dependence on extractor location. In Fig. 9a the peak transmission efficiencies of the in-line and lower extractor positions perform worse than the 0.4 mm and 0.5 mm position peak efficiencies. However, the results do show that transmission efficiency has a strong dependence on voltage with extractor positions above the emitter being more sensitive to increasing voltage than those extractor positions below the emitter.

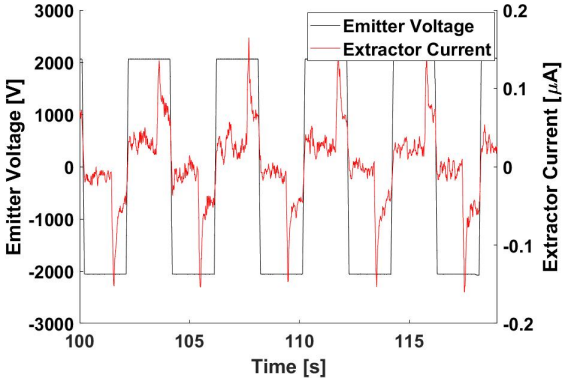

(a) Transient behavior of extractor current near the onset voltage for applied emitter voltage of 2060 V.

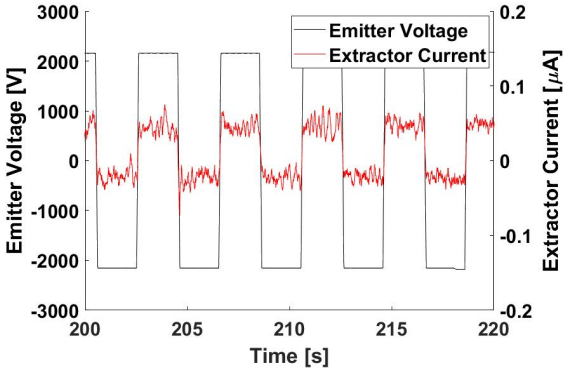

(b) Transient behavior of extractor current after the onset voltage for applied emitter voltage of 2160 V.

Fig. 10 Time-resolved extractor current plotted against time-resolved voltage showing the current behavior near onset with the extractor in-line with the emitter.

1. Transient Behavior

Time-resolved measurements of the extractor current near onset show similar results as the plume current, with a delay between applied potential and current on the extractor from impinging ions. An initial peak in the extractor current is also seen in Fig. 10a after the emission delay. Once the electric field is intense enough to immediately initiate emission at the Taylor cone the transient current peaks no longer occur and extractor current becomes stable. This behavior has implications for the lifetime and efficiency of porous electrosprays as emission sites that operate in this regime may be disproportionately contributing to performance losses.

V. Conclusion

An initial experimental campaign was completed examining the telemetry of a porous-media single emitter ionic liquid ion source as extractor-to-emitter distance was varied. Results showed a linear increase in onset voltage with increasing extractor-to-emitter distance. Discrete steps in the current followed by changes in the I-V slope indicated the onset of secondary and tertiary emission sites on the emitter. Extractor positions in-line with the emitter and below had noticeably higher overall I-V scaling compared to extractor positions above the emitter. No clear relationship between extractor position and transmission efficiency was determined. Formation of the tertiary site at downstream extractor positions did result in significantly higher extractor current than when the tertiary site formed at lower extractor positions. Transient behaviour of the extractor and plume current near onset voltage at downstream extractor positions was also examined. The decay rate in Δt between applied potential and emission was not affected by extractor position.

This work is being extended into a more complete experimental analysis of extractor-emitter geometry and alignment using a single emitter. The effects of centering alignment between the extractor orifice and emitter tip, orifice diameter, extractor-emitter tilt, and extractor-to-emitter distance have on transient current behaviour, onset voltage, beam divergence, ion energy distribution, and transmission efficiency will be characterized. The voltage where thruster operation reaches unstable regimes will also be used to determine the operating voltage envelope for a single emitter.

Acknowledgments

This work was supported by an Institute for International Education (IIE) Graduate International Research Experience (GIRE) fellowship under NSF grant no. 1829436. The Authors thank Dr. Ivan Arnold for manufacturing the borosilicate glass single emitter chips used during testing. The Authors would also like to thank Dr. Chengyu Ma, Szymon Dworski, and all lab members of the University of Southampton's David Fearn Laboratory for their informative conversations.

References

[1] Banerjee, S., and Mazumdar, S., "Electrospray Ionization Mass Spectrometry: A Technique to Access the Information beyond the Molecular Weight of the Analyte," *International Journal of Analytical Chemistry*, Vol. 2012, 2012, pp. 1–40. https://doi.org/10.1155/2012/282574.

[2] Levchenko, I., Bazaka, K., Ding, Y., Raitses, Y., Mazouffre, S., Henning, T., Klar, P. J., Shinohara, S., Schein, J., Garrigues, L., Kim, M., Lev, D., Taccogna, F., Boswell, R. W., Charles, C., Koizumi, H., Shen, Y., Scharlemann, C., Keidar, M., and Xu, S., "Space micropropulsion systems for Cubesats and small satellites: From proximate targets to furthermost frontiers," *Applied Physics Reviews*, Vol. 5, No. 1, 2018, p. 36. https://doi.org/10.1063/1.5007734, URL http://dx.doi.org/10.1063/1.5007734.

[3] Mennesson, B., "HabEx: Habitable Exoplanet Observatory Final Report," Tech. rep., Jet Propulsion Laboratory, Pasadena, CA, 2019.

[4] Demmons, N., Knott, J., Margousian, A., Fedkiw, T., and Alvarez, N., "Electrospray attitude control system flight preparation," *AIAA Science and Technology Forum and Exposition, AIAA SciTech Forum 2022*, 2022, pp. 1–13. https://doi.org/10.2514/6.2022-0039.

[5] Wirz, R. E., Collins, A. L., Thuppul, A., Wright, P. L., Uchizono, N. M., Huh, H., Davis, M. J., Ziemer, J. K., and Demmons, N. R., "Electrospray Thruster Performance and Lifetime Investigation for the LISA Mission," *AIAA Propulsion and Energy*, AIAA, Indianapolis, IN, 2019. https://doi.org/10.2514/6.2019-3816.

[6] Schroeder, M. R., Bruno, A. R., and Lozano, P. C., "Externally wetted ionic liquid electrospray transient emission characterization," *AIAA Science and Technology Forum and Exposition, AIAA SciTech Forum 2022*, 2022, pp. 1–11. https://doi.org/10.2514/6.2022-0037.

[7] Natisin, M. R., Zamora, H. L., McGehee, W. A., Arnold, N. I., Holley, Z. A., Holmes, M. R., and Eckhardt, D., "Fabrication and characterization of a fully conventionally machined, high-performance porous-media electrospray thruster," *Journal of Micromechanics and Microengineering*, Vol. 30, No. 11, 2020. https://doi.org/10.1088/1361-6439/abb8c3.

[8] Courtney, D. G., Dandavino, S., and Shea, H., "Comparing direct and indirect thrust measurements from passively fed ionic electrospray thrusters," *Journal of Propulsion and Power*, Vol. 32, No. 2, 2016, pp. 392–407. https://doi.org/10.2514/1.B35836.

[9] Brikner, N., and Lozano, P. C., "The role of upstream distal electrodes in mitigating electrochemical degradation of ionic liquid ion sources," *Applied Physics Letters*, Vol. 101, No. 19, 2012. https://doi.org/10.1063/1.4766293.

[10] Coffman, C. S., and Lozano, P. C., "On the Manufacturing and Emission Characteristics of Dielectric Electrospray Sources," *49th AIAA/ASME/SAE/ASEE Joint Propulsion Conference*, AIAA, San Jose, CA, 2013, pp. 1–12. https://doi.org/10.2514/6.2013-4035.

[11] Romero-Sanz, I., Bocanegra, R., Fernandez de la Mora, J., and Gamero-Castaño, M., "Source of heavy molecular ions based on Taylor cones of ionic liquids operating in the pure ion evaporation regime," *Journal of Applied Physics*, Vol. 94, No. 5, 2003, pp. 3599–3605. https://doi.org/10.1063/1.1598281.

[12] Huang, C., Li, J., Li, M., Si, T., Xiong, C., and Fan, W., "Experimental investigation on current modes of ionic liquid electrospray from a coned porous emitter," *Acta Astronautica*, Vol. 183, No. October 2020, 2021, pp. 286–299. https://doi.org/10.1016/j.actaastro.2021.03.014.

[13] Courtney, D. G., Wood, Z., Gray, S., and Model, J., "High-Speed Transient Characterization of the Busek BET-300-P Electrospray Thruster," *The 36th International Electric Propulsion Conference*, 2019, pp. 1–18.

[14] Courtney, D. G., and Shea, H., "Influences of porous reservoir Laplace pressure on emissions from passively fed ionic liquid electrospray sources," *Applied Physics Letters*, Vol. 107, No. 10, 2015. https://doi.org/10.1063/1.4930231, URL http://dx.doi.org/10.1063/1.4930231.

[15] Bruno, A. R., Schroeder, M. R., and Lozano, P. C., "Characterization of Electrospray Thrusters with HAN-Based Monopropellants for Multimode Propulsion Applications," *AIAA Science and Technology Forum and Exposition, AIAA SciTech Forum 2022*, 2022, pp. 1–12. https://doi.org/10.2514/6.2022-2490.

[16] Petro, E. M., Bruno, A. R., Lozano, P. C., Perna, L. E., and Freeman, D. S., "Characterization of the tile electrospray emitters," *AIAA Propulsion and Energy 2020 Forum*, 2020, pp. 1–13. https://doi.org/10.2514/6.2020-3612.

[17] Ma, C., Bull, T., and Ryan, C. N., "Time-of-Flight Characterization of Electrospray Thrusters Using Porous Emitters with High Emission Currents," *Journal of Propulsion and Power*, 2021, pp. 1–34.